



## 1. Introduction

A remote sensing satellite, FORMOSAT-5, was launched by a SpaceX Falcon 9 launch vehicle from Vandenberg Air Force Base Space Launch Complex 4E at 2:51 25 August 2017 CST into a 98.28° inclination sun-synchronous circular orbit at 720 km altitude along 1030/2230 local time (LT) sector. Advanced Ionospheric Probe (AIP) as shown in Figure 1 was proposed by Space Payload Laboratory, Graduate Institute of Space Science, National Central University under an announcement of opportunity for a piggyback science payload of the FORMOSAT-5 satellite and granted by National Space Organization (NSPO) in 2012. The payload was limited in mass under 5 kg, average power per orbit less than 5 W, and lifetime longer than 2 years in mission operation.

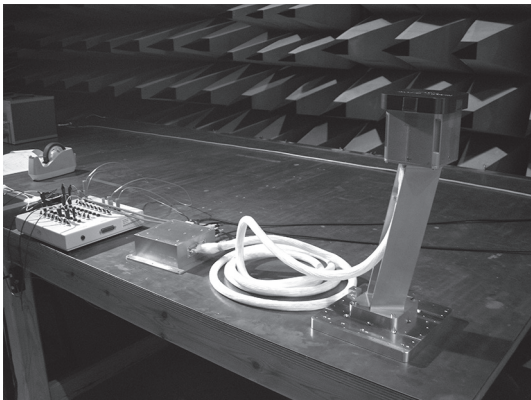


Figure 1: A photograph of the AIP flight model under electromagnetic compatibility test at National Space Organization

Note: The AIP sensor with a red cover is mounted on a stand in the right to enlarge field of view and a Science Payload Electronics Unit like a metal box in the left to control the sensor operation and communicate with a Command and Data Management Unit.

The AIP has heritages from past successful missions conducted by NCU and NSPO like Ionospheric Plasma and Electrodynamics Instrument (IPEI) onboard ROCSAT-1 satellite operated during 1999-2004, ion probe onboard Sounding Rocket V launched on 18 January 2006, and plasma probe onboard Sounding Rocket VII on 5 May 2010. After then, two

AIP sensors were installed on Space Plasma Sensor Package onboard Sounding Rocket IX and have completed a successful flight test on 26 March 2014. Note that the ion probe, the plasma probe, and an impedance probe on Space Plasma Sensor Package were designed and fabricated by Prof. Shigeyuki Minami, Osaka City University. The AIP has been verified its performance at lab, in a flight test on SR-IX, and during in-orbit checkout phase of the FORMOSAT-5 satellite. Hysteresis effect on measured I-V curves has been greatly reduced by sensor design and fabrication. The flight proven AIP is now in a two-year operation to explore space weather/climate and seismic precursors associated with strong earthquakes. The AIP has become the 1st Taiwan-made science payload onboard FORMOSAT satellites and successfully reached technical readiness level 9.

The AIP is basically a multi-grid planar ion probe integrated with a planar Langmuir probe within a 10 cm × 10 cm aperture as Figure 2. Unlike the other single-function plasma sensors, the AIP is a software-programmable sensor that plays various roles like Planar Langmuir Probe (PLP), Retarding Potential Analyzer (RPA), and Ion Drift Meter (IDM)/Ion Trap (IT) to maximize the total availability of ionospheric plasma concentrations, velocities, and temperatures.

The AIP has another feature in that it measures the total



Figure 2: A photograph of the AIP sensor

Note: The multi-grid ion probe entrance is at the center of the sensor and an electrode with a guarding ring of the planar Langmuir probe on the right bottom corner.

---

ion concentration at a sample rate up to 8,192 Hz. Using this sample rate, fine density structure of the equatorial plasma irregularities can be studied in comparison to the other on-duty plasma sensors like Special Sensor for Ions and Electrons (SSIIES) onboard Defense Meteorological Satellite Program (DMSP) satellites at 24 Hz and decommissioned sensors like IPEI onboard ROCSAT-1 satellite at 1,024 Hz and Instrument Analyseur Plasma (IAP) onboard Detection of Electro-Magnetic Emissions Transmitted from Earthquake Regions (DEMETER) satellite at 160 Hz.

## 2. Scientific objectives

The AIP is designed in total availability of ionospheric parameters and high sample rates to study space weather/climate like equatorial plasma irregularities, background ionosphere, and ionospheric disturbance caused by geomagnetic storm, and seismic precursors associated with strong earthquakes ionospheric perturbations as follows.

### 2.1 Equatorial plasma irregularities

One of the most important phenomena in the equatorial ionosphere is the generation of the equatorial spread F (ESF). It is expected that the ESF is related to plasma density irregularity structure caused by initial seeding perturbations from the large-scale gravitational Rayleigh-Taylor instability. The disturbed structure is generated at the bottom side of the F region and can be developed and extended to the topside ionosphere with very large gradient in plasma concentrations. These irregularities can seriously affect the propagation of radio waves over a large range of frequencies. Strong scintillations have been observed from high frequency to GHz frequency range. Therefore, the statistical survey of the global distributions of the ionospheric density irregularities is very important. These patterns have been investigated in a macro-level approach with AE-E spacecraft observation and with ROCSAT-1/IPEI data in the last two decades. The FORMOSAT-5/AIP will continue the previous studies to examine the long-term trend of these patterns in this decade.

In a micro-level approach, the AIP is capable of measuring the equatorial plasma irregularities up to 8,192 Hz and then analyzing the spectral behaviors on total ion concentration and drift velocity. It may be helpful to re-examine the frozen-in approximation in the ionosphere with the limited regime of scale length between the Boltzmann relation and non-Boltzmann relation.

### 2.2 Background ionosphere

Ion parameter global distributions were derived from the ROCSAT-1 observation and revealed many unique features in various local time sectors, like pre-dawn heating, ion temperature crests in the morning hours, and movements of the temperature crests in the afternoon sector, etc. However, lack of electron temperature measurement in the ROCSAT-1 satellite, many temperature features could not be fully understood.

In the early stage of the AIP mission, the instrument will be

routinely operated within  $\pm 60^\circ$  latitude in the night-side sector (2230 LT sector) to meet a 5-W limit in average power per orbit. Some well-known nighttime ionospheric features like temperature crests and troughs have been detected by the OGO6 and the DMSP spacecraft over the last several decades. A model study for the DMSP ion temperature measurement has confirmed that the temperature crests observed at near  $15^\circ$  latitude in the winter hemisphere are due to adiabatic heating and the troughs observed near the magnetic equator are due to adiabatic cooling as plasma is transported along the magnetic field from the summer hemisphere to the winter hemisphere in the nighttime topside ionosphere. The upcoming AIP data will make it possible to construct the ion parameter global distributions to investigate the phenomena.

### 2.3 Ionospheric disturbance by geomagnetic storm

During geomagnetic storm time, prompt penetration of electric fields and long-lasting disturbance dynamo effect results in large-scale plasma motion in the ionosphere. An observation of large density depletion in a narrow longitude near the South Atlantic Anomaly (SAA) region by DMSP F9 satellite was reported at 840 km altitude during the March 1989 magnetic storm. The density depletion was attributed to an enhanced equatorial fountain effect from a locally enhanced eastward electric field near the SAA region related to a large energetic particle precipitation during the storm. It is interesting that similar observations of large density depletion events were again observed during the 6-7 April 2000 and the 15-16 July 2000 magnetic storms by ROCSAT-1 satellite, at 600 km altitude traversing the magnetic flux tube in the east-west direction. The 15-16 July events were reported to correlate with the SAA region. The large density dropout was further classified in two groups of ESF plasma irregularities that occurred in either side of the midnight meridian during the storm recovery phase. The two groups of ESF plasma irregularities were both observed in the neighborhood of the SAA region. The FORMOSAT-5/AIP can make a similar observation at 720 km altitude to monitor these plasma disturbances in a very high resolution during the geomagnetic storm. However, it is also noted that such kind of great geomagnetic storms may occur rarely in a solar activity decline phase of during the FORMOSAT-5 mission lifetime.

### 2.4 Seismic precursor

Recently ionospheric electron temperatures observed by HINOTORI satellite were further examined during three earthquakes; M6.6 occurred in November 1981, M7.4 and M6.6 in January 1982 over the Philippines, respectively. It was found that the electron temperature around the epicenters significantly decreased in the afternoon periods within 5 days before and after the three earthquakes. The AIP has a great advantage in measuring electron temperature but also more ion parameters will be cross-checked for possible mechanism correlation.

Meanwhile, the FORMOSAT-5 satellite will pass over Taiwan every two days and the AIP can also collaborate with integrated Study for Taiwan Earthquake Precursors (iSTEP) to survey all possible earthquake precursors for disaster reduction.

To see whether FORMOSAT-5/AIP can be used to detect seismo-ionospheric precursors (SIPs) or not, ion density, temperature, and velocity probed by ROCSAT-1/IPEI have been examined as well as the global ionospheric map (GIM) of the total electron content (TEC) derived by ground-based GPS receivers during the 31 March 2002 M6.8 Earthquake in Taiwan. The anomalous decreases in the ROCSAT-1/IPEI ion density and the GIM TEC concurrently appear around the epicenter area 1-5 days before the earthquake, which suggests that FORMOSAT-5/AIP can be used to detect SIPs.

### 3. Principles of measurement

The AIP is an all-in-one plasma sensor to measure all the characteristics of the ionospheric plasma in operation modes like the PLP, RPA, and IDM/IT but in a time-sharing way.

#### 3.1 PLP

When the AIP operates in the PLP mode, the PLP electrode (shown in the left of the Figure 3) is applied to a sweeping voltage between  $-10\text{ V}$  and  $+10\text{ V}$  and isolated from aperture plane. Once the sweeping voltage is lower than plasma potential, the electrode repels electrons and accelerates ions. As the voltage decreases, electron current decreases rapidly. The electron temperature ( $T_e$ ) can be determined by the slope of the current-voltage ( $I$ - $V$ ) curve as shown in Eq. (1),

$$\frac{kT_e}{e} = \frac{1}{\frac{d}{dV} [\ln(I)]}, \quad (1)$$

where  $I$  is the total electric current through the PLP electrode,  $V$  is the sweeping voltage applied to the PLP electrode,  $k$  is the Boltzmann constant,  $e$  is the electron charge. As the slope of the  $I$ - $V$  curve is flat, the  $T_e$  is higher. As the slope is steep,

the  $T_e$  is lower.

#### 3.2 RPA

The AIP multi-grid ion probe consists of four high-transparent electroformed gold grids to manage incoming plasma, as shown in Figure 3. The first dual grids, G1, are aperture grids arranged in the front of the probe and connected to a floating potential device that allow the incoming plasma to flow smoothly into the probe without interference from the transverse electric field. The second grid, G2, is a retarding grid connected to a programmable sweeping retarding voltage circuit between  $-10\text{ V}$  and  $+10\text{ V}$ . The grid forms an electric potential barrier to block low energy positive ions from the probe. The third grid, G3, is a suppressor grid maintained at  $-15\text{ V}$  to repel the incoming electrons into a quadrant gold-coating collector and can also reduces the amount of photoelectrons escaping from the collector when the sun-rays strike on the collector. All four quadrant collector gold-coating plates are maintained at the floating potential and are programmable to connect with an ammeter or individual ammeters via an analog switch.

In the RPA mode, positive ions with low kinetic energy are repelled out of the probe or neutralized by the grids and probe interior boundary as the retarding voltage increases. Positive ions with high kinetic energy can penetrate through the retarding grid to the collector if they do not contact with the suppressor grid or the interior probe boundary. The higher the retarding voltage, the lower the current is measured at the collector. Such a sampling process can be recorded as the  $I$ - $V$  curves to derive the ion temperature, composition, and ion ram speed. A 1-dimensional ion current equation for this application is written in Eq. (2),

$$I(V) = A \sum_i q_i N_i U_i \frac{1}{2} \left[ 1 + \operatorname{erf}(\beta_i F_i) + \frac{\exp(-\beta_i^2 F_i^2)}{\sqrt{\pi} \beta_i U_i} \right], \beta_i = \sqrt{\frac{M_i}{2kT_i}}, \text{ and } F_i = U_i - \sqrt{\frac{2q_i V}{M_i}} \quad (2)$$

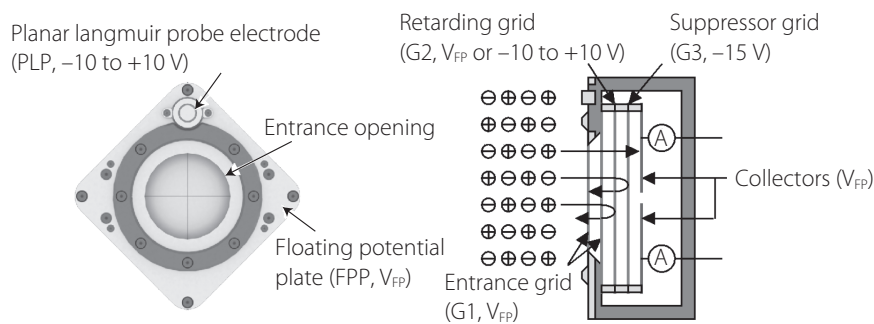


Figure 3: An illustration of the AIP to operate in the RPA mode

Note: Positive ions with low kinetic energy are repelled by a retarding grid biased at a voltage higher than plasma potential, but positive ions with high kinetic energy can penetrate through the retarding grid to the collector. Electrons are all repelled by a suppressor grids biased in  $-15\text{ V}$ .

where  $I$  is the ion current measured at the collector,  $q_i$  is the electric charge for species  $i$ ,  $A$  is the effective collection area of the collector,  $N_i$  is the ion concentration for species  $i$ ,  $U_i$  is the ion ram speed for species  $i$ ,  $M_i$  is the ion mass for species  $i$ ,  $\kappa$  is the Boltzmann constant,  $T_i$  is the ion temperature for species  $i$ ,  $V$  is the maximum electric potential along the path for plasma from outside environment to the probe (sometimes can be simplified as retarding potential). The electric potential is referenced to far-away plasma and it is assumed that the electric potential of the far-away plasma is zero. It is also noted that a numerical model to estimate the effects of grid alignment and electric potential depression on the grids is required to derive the precise  $T_i$  and  $U_i$ .

### 3.3 IDM/IT

In the IDM/IT mode, the G1 and the G2 are maintained at the floating potential. In the IT mode, all the four quadrant collector gold-coating plates are connected together with an ammeter. In the IDM mode, all the plates are connected with individual ammeters. The incoming ion arrival angles can be estimated from ion current differences in the adjacent ammeters, as shown in Figure 4. The arrival angle,  $\alpha$ , of the incoming ion for a circular aperture opening is expressed in Eq. (3),

$$\alpha = \tan^{-1} \left[ \frac{W}{2D} \cos \frac{\theta}{2} \right] \text{ and } \theta = \sin^{-1} \left[ 1 - \frac{(I_1 - I_2)}{(I_1 + I_2)} \right] \pi, \quad (3)$$

where  $W$  is the width of the aperture,  $D$  is the depth between the aperture and the collector. The immediate parameter  $\theta$  must be solved by numerical methods, e.g. fixed-point iteration. Note that the formula is a new starting point for a drift meter to use the circular aperture opening instead of the square aperture opening as before.

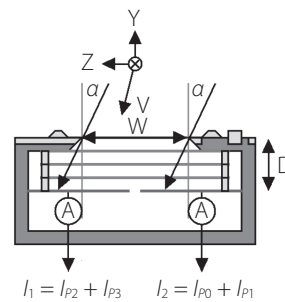
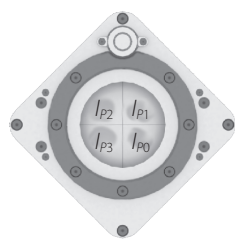


Figure 4: An illustration of the AIP to operate in the IDM mode

Table 1: AIP data rates for all parameters

Rates	IT ( $N_i$ )	IDM ( $\alpha_H$ and $\alpha_V$ )	PLP ( $T_e$ ) or RPA ( $T_i$ , $C_i$ , $U_i$ )	PRI ( $T_e$ , $T_i$ , $C_i$ , $V_i$ , $N_i$ )
NORMAL	128 Hz	32 Hz	1 Hz	1/3 Hz
FAST	1,024 Hz	256 Hz	1 Hz	1/3 Hz
BURST	8,192 Hz	2,048 Hz	1 Hz	1/3 Hz

### 3.4 Geophysical parameters

The AIP can be configured to measure ambient plasma at three sample rates, NORMAL rate operating at 128 Hz, FAST rate at 1,024 Hz, and BURST rate at 8,192 Hz. By default, the AIP is set to PRI (an initial point for PLP-RPA-IDM/IT) mode to measure ionospheric plasma in PLP, RPA and IDM/IT cycle mode at one second each sequentially. Therefore, it must be assumed that all ionospheric parameters have a slow temporal variation within 3 seconds as shown in Table 1 and are uniform within 22.5 kilometers in spatial scale (if the satellite speed is  $7.5 \text{ km s}^{-1}$ ). After one cycle is complete, the geophysical parameters,  $N_i$ ,  $V_i$ ,  $T_i$ , and  $T_e$ , can be derived from the steps shown in Figure 5. The AIP can also run PLP, RPA, or IDM/IT solely to increase the data rates for specific parameters as shown in Table 1, but this leads to an incomplete data set.

The PLP mode can obtain  $T_e$  directly.  $T_e$  will be used to estimate floating potential to obtain retarding potentials (referenced to plasma potential) with the retarding voltages (referenced to floating potential). The RPA mode can obtain  $T_i$ ,  $U_i$ , and  $C_i$  (composition ratio for species  $i$  to total ions). The IDM/IT mode can not only obtain the total ion flux and fur-

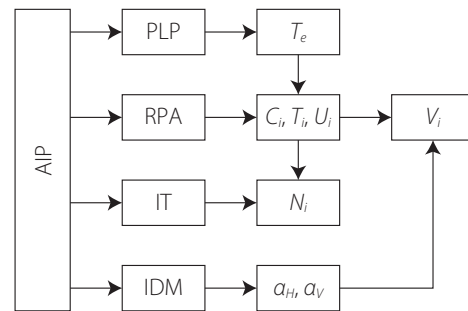


Figure 5: Geophysical ionospheric parameters derived from the AIP operation under PLP, RPA, and IDM/IT

ther convert to  $N_i$  with  $T_i$ ,  $U_i$ , and  $C_i$ , but also obtain two arrival angles,  $\alpha_H$  and  $\alpha_V$ , and convert them to  $V_i$  with  $U_i$ .

Under the FORMOSAT-5 satellite orbits the geophysical measurement requirements are derived from the International Reference Ionosphere model and listed in Table 2. The AIP is designed to outperform the geophysical measurement requirements of the FORMOSAT-5 satellite and its performance capabilities are listed in Table 3 for references.

#### 4. Evaluation on hysteresis in I-V curves

The “hysteresis” phenomenon in Langmuir probe I-V characteristics was observed in an article published in 1952 that the I-V curve collected by probe voltage ramp up is different from that by ramp down. The hysteresis is attributed to electrode surface contamination and can be reduced using a clean probe or by a rapid sweep of the probe voltage. Moreover, this is not just found in the Langmuir probe, it also happens to a multi-grid retarding potential analyzer that measures ion temperature. The plasma temperature cannot be correctly determined if significant hysteresis is shown in the I-V curve.

From the measurement principles, the grids inside the ion probe are used to provide electric potential surface to filter out unwanted charged particles. In the past, woven stainless steel grids were used, like the ion probe for the Sounding Rocket V and plasma probe for the Sounding Rocket VII. Sometimes the grids are further gold coated, as in ROCSAT-1/IPEI. The AIP uses electroformed gold grids to ensure better structure and strength in addition to higher transparency. In theory the electroformed grids can approximate ideal electric potential surfaces better than the woven grids for the same wire diameter and mesh density.

Meanwhile, laboratory simulation has been performed on an

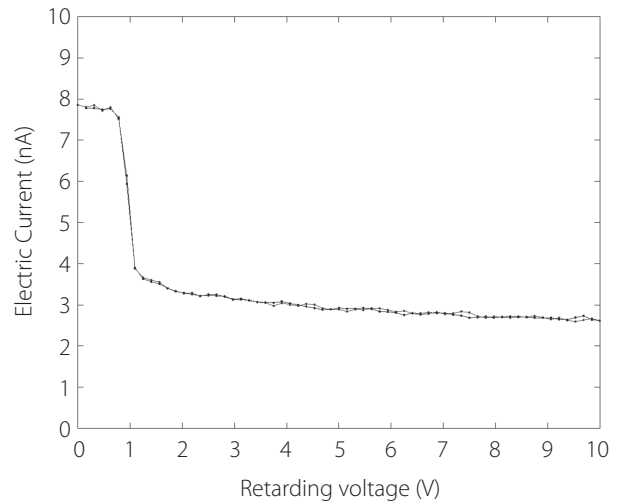


Figure 6: Two electric current-voltage curves measured by an AIP prototype in a plasma injection test

Note: The red line indicates the electric current measured when the retarding voltage of the G2 is sweeping up and the blue line when the retarding voltage is sweeping down.

AIP prototype in Space Plasma Simulation Chamber. Two I-V curves were measured by the AIP for retarding G2 sweeping up and down voltage in Figure 6 to verify the AIP measurement accuracy. It is clear that the two curves are almost identical and implies that the AIP electroformed gold grids can greatly reduce hysteresis in the measured I-V curves. Note also that the derived ion temperature is about 540 K using a grid-search curve fitting scheme.

#### 5. Preliminary flight results

After a long delay caused by a SpaceX Falcon 9 explosion at Cap Canaveral Air Force Station Space Launch Complex 40 during AMOS-6 static fire test on 1 September 2016, the

Table 2: FORMOSAT-5 geophysical measurement requirements

Parameters	Range	Sensitivity	Accuracy
$C_i$	5 % to 100 %	1 %	10 %
$N_i$	$10^3$ to $5 \times 10^6$ cm <sup>-3</sup>	1 %	10 %
$V_i$	$\pm 2$ km s <sup>-1</sup> (cross track) $\pm 2$ km s <sup>-1</sup> (ram)	$\pm 10$ m s <sup>-1</sup> $\pm 100$ m s <sup>-1</sup>	$\pm 50$ m s <sup>-1</sup> $\pm 200$ m s <sup>-1</sup>
$T_i$	750 to 5,000 K	$\pm 50$ K	$\pm 200$ K
$T_e$	750 to 5,000 K	$\pm 50$ K	$\pm 200$ K

Table 3: AIP performance capabilities

Parameters	Range	Sensitivity	Accuracy
$C_i$	3 % to 100 %	1 %	10 %
$N_i$	$4 \times 10^2$ to $1.2 \times 10^7$ cm <sup>-3</sup>	1 %	10 %
$V_i$	$\pm 3.2$ km s <sup>-1</sup> (cross track) $\pm 5$ km s <sup>-1</sup> (ram)	$\pm 10$ m s <sup>-1</sup> $\pm 100$ m s <sup>-1</sup>	$\pm 50$ m s <sup>-1</sup> $\pm 200$ m s <sup>-1</sup>
$T_i$	500 to 10,000 K	$\pm 50$ K	$\pm 200$ K
$T_e$	500 to 10,000 K	$\pm 50$ K	$\pm 200$ K

FORMOSAT-5 was finally launched on 25 August 2017 CST. The AIP was powered on in orbit first time on 7 September 2017. The initial sensor and SPEU temperature is  $-20^{\circ}\text{C}$  and  $0^{\circ}\text{C}$ , respectively. After a two-month in-orbit checkout phase, the AIP is now in a two-year routine operation and collects around 80 MBytes FAST rate science data everyday.

Here we select three I-V curves measured in RPA/IPTON/FPD-OFF mode at 2:36 24 September 2017 UT shown in Figure 7 for examples. These I-V curves are almost free of contamination. However, a very negative satellite ground potential was found in 2-3 V less than ambient plasma potential. The abnormal ground potential will impact original data processing plan severely and a careful evaluation shall be considered to finalize the data processing.

Meanwhile, a preliminary ion saturation current profile with uncertainty estimate (shown in Figure 8) was measured by FORMOSAT-5/AIP along geographic longitudes near  $315^{\circ}$  with a geographic latitude coverage from  $-60^{\circ}$  to  $48^{\circ}$  during 01:30-2:00 19 September 2017 UT. There was no ESF found at this moment. An ion current maximum was shown near geo-

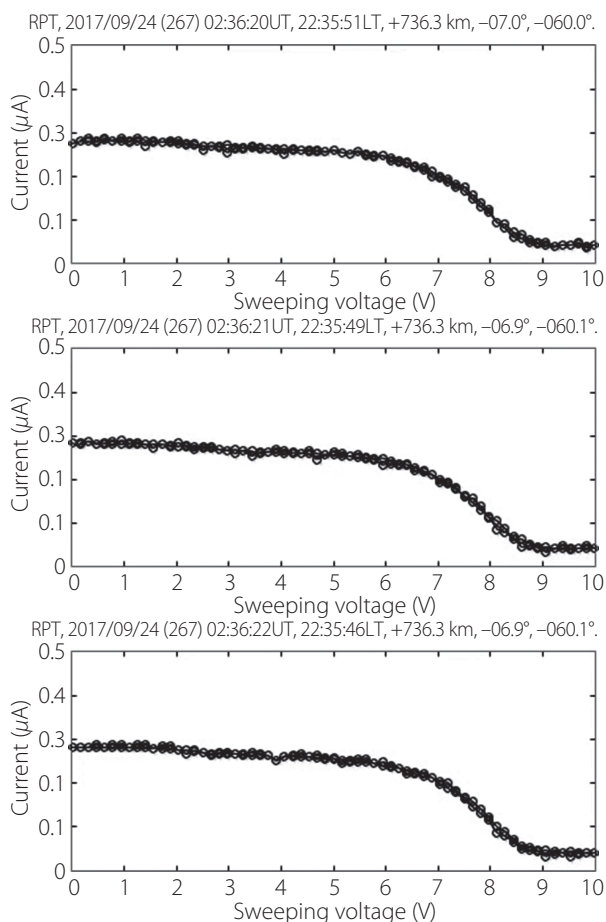


Figure 7: Three preliminary electric current-voltage curves measured by the FORMOSAT-5/AIP on 24 September 2017 during in-orbit check phase

Note: It is clear that these curves are almost free of contamination.

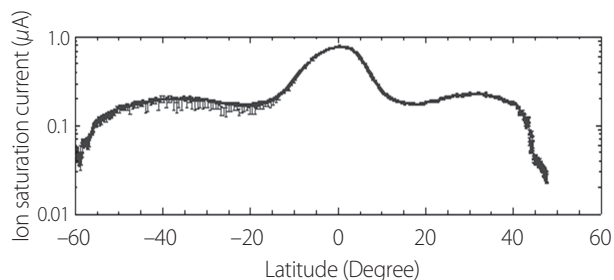


Figure 8: A preliminary ion saturation current profile measured by the FORMOSAT-5/AIP with uncertainty estimates along geographic longitudes near  $315^{\circ}$  with a geographic latitude coverage from  $-60^{\circ}$  to  $48^{\circ}$  during 1:30-2:00 19 September 2017 UT

Note: An ion current maximum near geographic equator corresponds to an ion density peak at  $5 \times 10^5 \text{ # cm}^{-3}$ .

graphic equator and corresponds to an ion density peak at  $5 \times 10^5 \text{ # cm}^{-3}$ . Mid-latitude troughs could be found near  $-55^{\circ}$  and  $45^{\circ}$  geographic latitude. These features are quite well known and understood to help identify the AIP performance.

## 6. Summary

The AIP is designed to maximize total availability in ionospheric plasma parameters and sample rates to meet the scientific objectives. The I-V curves measured by the AIP in laboratory and in space indicated that the ion sensor is almost free of contamination. Now the AIP team is on-going data processing and expects accurate ionospheric plasma parameters are soon available for scientific research and application. The scientific objectives outlined in this article will be finally clarified in the future.

Once comprehensive dataset is available from the AIP, a systematic examination of longitudinal and seasonal variations in the ionospheric parameters in the topside F region can be conducted for all latitudinal coverage. The transient and long-term variations in ionospheric plasma can be monitored in a solar activity decline phase and benefit the public and scientists who are interested in space weather/climate as well as the seismic precursors associated with strong earthquakes.

## Acknowledgements

This work was supported by grant NSPO-S-100005 National Space Organization, National Applied Research Laboratories, Taiwan, ROC. The author wants to deeply appreciate Prof. Shigeyuki Minami's help. Without his kindly instructions on payload and plasma chamber, it is impossible for NCU to make AIP work. Note also that this article is mainly modified from an article "Lin, Z. W., C. K. Chao, J. Y. Liu, C. M. Huang, Y. H. Chu, C. L. Su, Y. C. Mao, and Y. S. Chang (2017), Advanced Ionospheric Probe scientific mission onboard FORMOSAT-5 satellite, *Terr. Atmos. Ocean. Sci.*, doi: 10.3319/TAO.2016.09.14.01(EOF5)".